Ahamed Fayeez Tuani[1],
Siva Kumar Subramaniam[1,*],
Vigneswara Rao Gannapathy[1],
Siti Aisyah Anas[1],
R. Sujatha[2]

Frequency Sweeping Approach for Achieving Optimal Resonance Frequency in Inductive Wireless Power Transmission (IWPT)

Journal of Electrical Systems

Abstract: Wireless Power Transmission (WPT) technology is widely used but faces significant efficiency limitations due to reliance on manual tuning methods when the load changes. It also requires precise alignment between the transmitter and receiver coils typically confined to distances of less than a few centimeters. Moreover, load variations disrupt the magnetic resonance requiring manual adjustments to restore efficiency. This tuning process is often tedious and inaccurate which leads to suboptimal performance ultimately reducing transmission efficiency. The frequency sweep technique was employed to continuously align the operating frequency with the resonant frequency. This study presents a comprehensive approach for determining the optimal operating frequency in inductive WPT systems enabling the development of an automatic adaptive tuning technique. Experiments were conducted with an Arduino-based model representing the WPT system. Results demonstrated that transmission efficiency increased by at least 10% at a four-centimeter coil separation when the operating frequency was correctly aligned with the resonance frequency. These findings underscore the potential for substantial efficiency improvements in WPT systems through automatic tuning methods offering a more reliable and precise solution compared to manual tuning.

Keywords: Resonance Frequency, Mutual Inductance, Inductive WPT, Wireless power transmission (WPT)

1. INTRODUCTION

Wireless power transmission also known as wireless power transfer (WPT) is a system that allows the transmission of electrical energy between sources and devices without any physical connection by relying on coupling components which are the transmitter and receiver. This technology has made charging devices remotely a more convenient solution than the conventional wired system [1]. Examples of current applications using this technology are automated material handling systems (AMHS) [2], implant medical devices [3], battery charging applications [4] and many more. WPT can be traced back to the pioneering work of Serbian-American inventor and electrical engineer Nikola Tesla during the late 19th century. Tesla's investigations focused on the development of systems capable of transmitting electrical energy over long distances using large electrical towers [5]. Figure 1 illustrates how charged particle fields are used to transfer energy between transmitters and receivers over an air gap. After being converted into an oscillating field and transported through the air, the energy is finally received by a receiver and converted into a useful electrical current. However, one of the fundamental challenges in IWPT systems is the dynamic nature of the load which can cause variations in the system's resonance frequency hence requiring constant adjustments of the operating frequency to realign with the resonance point. Traditionally, these adjustments are performed manually through tuning techniques, a method that is both time-consuming and prone to inaccuracies.

[1] * Corresponding author: Ahamed Fayeez Tuani, Fakulti Teknologi & Kejuruteraan Elektronik & Komputer, Universiti Teknikal Malaysia Melaka, Jalan Hang Tuah Jaya, 76100 Durian Tunggal, Melaka, Malaysia E-mail: fayeez@utem.edu.my
1 Fakulti Teknologi & Kejuruteraan Elektronik & Komputer, Universiti Teknikal Malaysia Melaka, Jalan Hang Tuah Jaya, 76100 Durian Tunggal, Melaka, Malaysia
2 Department of Embedded Technology (IoT and sensors specialization), Vellore Institute of Technology, Tiruvalam Rd, Katpadi, Vellore, Tamil Nadu 632014, India

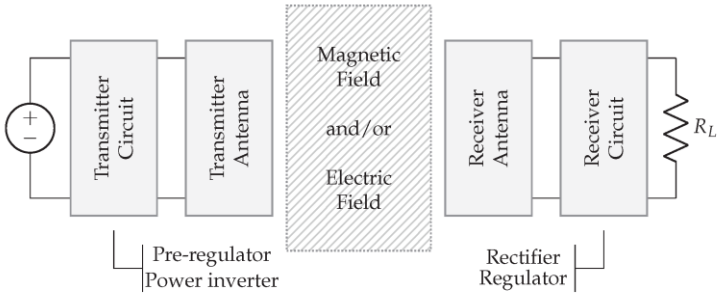

Figure 1: Diagram of a general Wireless Power Transmission system.

The manual process often results in suboptimal tuning leading to significant losses in transmission efficiency and unreliable power transfer performance. Furthermore, as the distance between the transmitter and receiver coils increases or as environmental conditions fluctuate, maintaining the resonance becomes even more complex. The inability to continuously monitor and adjust the frequency as load conditions change exacerbates this problem. The lack of a robust, adaptive tuning mechanism hinders the system's ability to dynamically compensate for changes resulting in inefficient power transfer, heat dissipation and degraded system performance. Addressing this problem requires an automatic tuning approach capable of real-time adjustments, ensuring that the operating frequency consistently aligns with the changing resonance conditions for optimal power transfer. The objective of the study is to enhance the efficiency of IWPT systems by identifying the ideal operating frequency that corresponds with the resonant frequency therefore facilitating the development of a self-adaptive methodology. Frequency sweep analysis is conducted to assess the performance of the IWPT system and determine the frequency that optimizes power transmission efficiency. This offers essential insights required for the creation of a self-adaptive tuning mechanism later on which will be capable of dynamically adjusting the operating frequency in real-time hence assuring continuous resonance and optimum power transmission without operator intervention. A frequency sweep is a process used to identify the optimal operating frequency where maximum power transfer occurs. In this paper, the aforementioned method, which could estimate the frequency for the IWPT system with parameters only from the transmitter side itself and maximize the transmitted power, is applied to investigate and estimate the optimal frequency of the IWPT setup. The proposed method is related to the theoretical formula of magnetically coupled circuits, which estimates the value of mutual inductance and accounts for the total inductance of the system to calculate the estimated resonant frequency [6].

2. PREVIOUS WORK

Through recent research, most methods used to optimize IWPT systems are synchronous series compensator [7], Automatic Resonant Frequency Tuning System (ATAC) [8], [9]-[11], phase-shift keying modulation technique [12], Power Factor Correction (PFC) boost converter [13], phase adjustment [14], Inductor-Capacitor-Capacitor (LCC) compensation topology [15] and a lot more. However, these methods would involve additional circuits to the system such as adjustable capacitors which increase the cost and complexity of the system. Not only that, these methods would require the operating frequency of the system to be fixed while the receiver side was focused on matching frequency to the transmitter side. Having said that, determining the resonant frequency is still the main key to achieving optimal efficiency in the IWPT system [16]. Moreover, there is a lack of study about optimizing the power transmission of transmitters via updating resonant frequency.

Generally, two main methods have been explored by researchers to achieve resonance frequency. The first method keeps the supply frequency constant and adjusts the reactive elements of the coils or compensation networks [17, 18, 19]. For instance, one approach involves adding an extra coil to the receiving coil to change its reactance and maximize the voltage applied to the load [17]. Another technique adjusts the inductance of the transmitting coil by controlling the DC in an additional coil wound on the same core [18]. Yet another method uses several capacitors that can be selectively connected in parallel to the main capacitor through electronic switches to achieve resonance on the transmitting side [19]. Unlike these solutions, the method presented in this paper does not need additional coils or capacitors, making the implementation of the IWPT simpler.

The second method involves varying the supply frequency. One study uses a closed-loop control of the current amplitude in the transmitting coil, with the theoretical resonance amplitude as a reference and the supply frequency as the manipulated variable [20]. Similarly, a real-time closed-loop approach is used in an RF IPTS, adjusting the supply frequency between 40 MHz and 120 MHz to minimize the fraction of the RF signal reflected from the transmitter [21]. The core research gap lies in the inability of these methods to efficiently and dynamically adjust to changing loads in real-time, thus maintaining optimal resonance without manual intervention. The need for a more adaptive, self-tuning system that can continually monitor and adjust the operating frequency in real-time, without relying on additional hardware, is evident. To solve the aforementioned gap in research, the proposed approach performs a frequency sweep analysis to evaluate the efficiency and effectiveness of the inductive power transmission system by analyzing the transmitted power by comparing the performance based on resonant frequency and estimated frequency, aiming to optimize the power transmission process via self-adaptive tuning which is not covered in this paper.

3. METHODOLOGY

The flowchart in Figure 2 outlines a comprehensive methodology for analyzing the resonance frequency of the IWPT proposed in this study. The process begins with Phase 1 where the objective is to develop an inductive wireless power transmission prototype. This involves designing the physical IWPT system, including the transmitter and receiver coils, a resonant tank circuit with capacitors and inductors for achieving magnetic resonance, and a PWM-controlled power supply to modulate the frequency of the input signal. The prototype serves as the hardware basis for the study, and the initial system setup includes ensuring the basic inductive coupling between the coils, which is vital for efficient power transfer.

Following the construction of the prototype, Phase 2 transitions into simulation, where the same IWPT circuit is replicated in Proteus simulation software. This step is crucial for validating the design before physical implementation. The simulation aims to emulate the physical system's behavior, adjusting for coil distances, input frequencies, and power transfer efficiency. It includes checking for consistency between the simulation and the hardware prototype by comparing the voltage, current, and power values obtained from both sources. Ensuring the simulation's accuracy helps minimize potential hardware-related issues and establishes a solid foundation for subsequent experimentation.

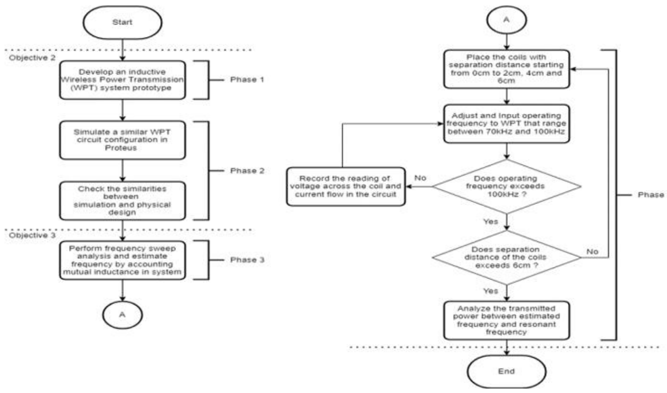

Figure 2: Flowchart of the experimental methodology

Moving into Phase 3, the project focuses on the frequency sweep analysis to explore how variations in coil separation affect the resonance frequency and power transfer efficiency. This phase involves placing the transmitter and receiver coils at various separation distances—starting from 0 cm and gradually increasing to 2 cm, 4 cm, and 6 cm. As coil separation increases, the mutual inductance between the coils decreases, leading to a shift in the resonant frequency and a reduction in power transfer efficiency. The frequency sweep process entails adjusting the input frequency of the transmitter between 70 kHz and 100 kHz, a range that encompasses the expected resonant frequency for this system. At each frequency step, voltage and current readings are taken to observe the system’s behavior at different frequencies. This step is crucial in identifying the resonant frequency where maximum power transfer occurs, as this frequency is where the inductive reactance and capacitive reactance are balanced, resulting in minimal impedance and efficient power transfer. A decision point follows, where if the operating frequency exceeds 100 kHz or the coil separation exceeds 6 cm, the sweep ends for the current set of conditions. Otherwise, the process continues with further measurements. Finally, Step 3 of Phase 3 analyzes the transmitted power at both the resonant frequency and the estimated frequency, comparing the power levels at these frequencies. This analysis aims to identify how well the system maintains efficiency despite variations in coil separation and other system parameters. The data collected throughout this process provides valuable insights into the system’s performance and the correlation between coil separation, frequency shifts, and power transfer efficiency. The frequency sweep itself, along with the comparisons between simulation and hardware, directly aligns with the project's aim to study the resonance frequency of IWPT systems. This methodology helps ensure that the system operates at its most efficient state, with optimal resonance achieved despite any changes in environmental or physical conditions.

The proposed WPT system comprises an Arduino Nano v3.0 board, half-bridge driver (IR2184PBF), MOSFET transistor (IRF740) as the inverter and RLC circuit. Figure 3 shows the complete circuit configuration for the proposed IWPT analysis. The Arduino Nano v3.0 was chosen for its compact size, ease of programming, PWM capabilities, low power consumption and cost-effectiveness thus making it ideal for controlling and optimizing the WPT system.

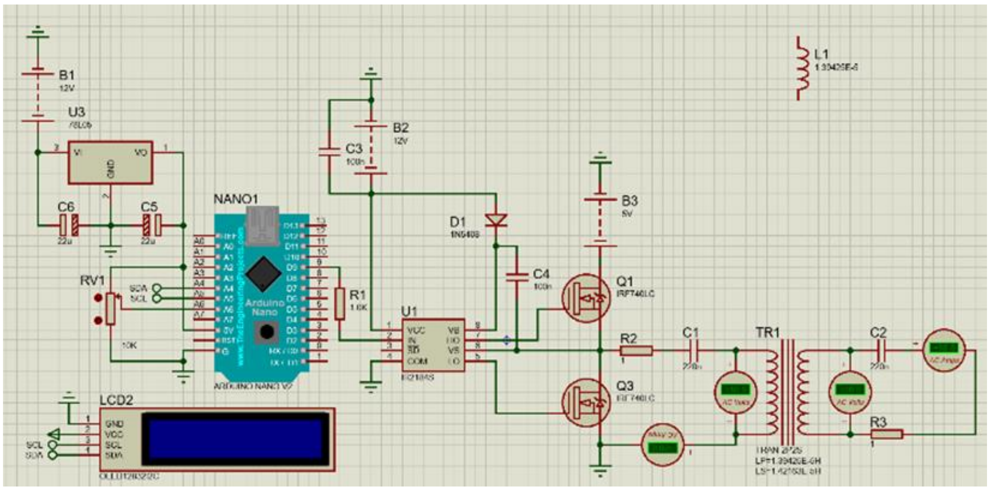

Figure 3: Circuit Configuration.

These components as shown in Figure 3 are chosen to make a simple AC squared wave supply whereas the Arduino Nano board acts as the main component to send the PWM signal towards the input signal of the half-bridge driver which then controls the timing of the switching devices (MOSFET transistor) or the inverter based on the given PWM signal from Arduino Nano board. Next, the inverter built with two MOSFET transistors generates an AC squared waveform from a DC power supply by switching according to the frequency of the PWM signal. For safety measurement, a 5V DC power supply was used on the drain voltage (or supply voltage) of the inverter. Once the AC squared wave supply was completed, the RLC circuit would be directly connected to the output of the inverter as the inductive power transmission system and the complete development is shown in Figure 4. The receiver side is a simple RLC circuit that consists of a resistor, inductor and capacitor in series configuration. In addition, some optional components were used in the prototype for specific features such as a potentiometer with 10kΩ for ADC values to allow the user to tune the frequency manually and SSD1306 OLED module that is used to display the current operating frequency.

Figure 4: Hardware Design of Inductive

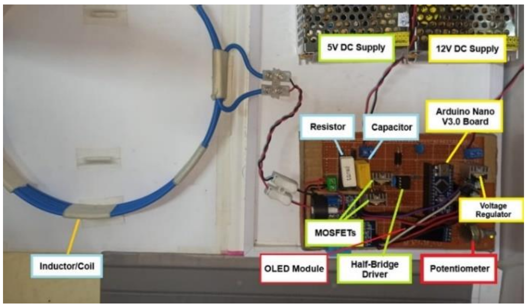

Table 1: Coil Design

Conductor Material	Annealed Copper
Cross Sectional Area of the wires	2.5 mm^2
Core Strands	7/0.67 mm
Current Rating	28 A
Voltage Rating	600 V
Number of Turns	6
Radius	10 cm
Solenoid length	2 cm

Power Transmission System.

Other than that, the handmade inductors for the transmitter and receiver were constructed using PVC-insulated power cable wire as it is cheaper than pure copper wire, flexible, has good insulation and is safer to experiment. However, the specification of the coils is shown in Table 1. Meanwhile, Table 2 indicates the inductance values that will be used later which were measured by using an LCR meter.

Table 1: Measurement of the Inductors, L1 and L2 (Coils)

f (kHz)	L1 (H)	Q1	L2 (H)	Q2	L1 AVG (H)	L2 AVG (H)
1.0	1.43E-05	0.1849	1.45E-05	0.1816	1.44E-05	1.46E-05
	1.44E-05	0.1853	1.46E-05	0.1877		
10.0	1.40E-05	1.774	1.43E-05	1.818	1.40E-05	1.43E-05
	1.40E-05	1.783	1.43E-05	1.81		
50.0	1.38E-05	8.4	1.40E-05	8.509	1.38E-05	1.41E-05
	1.37E-05	8.348	1.41E-05	8.543		
100.0	1.36E-05	15.44	1.40E-05	15.8	1.37E-05	1.40E-05
	1.37E-05	15.51	1.40E-05	15.83		
Average					1.394E-05	1.423E-05

The coupling coefficient of the system will be calculated for the hardware prototype with different separation distances between coils like 0cm, 2cm, 4cm and 6cm. To calculate the coupling coefficient, the value of mutual inductance, M is calculated using equation (1) where induced voltage is the voltage across the secondary coil and ω is the angular frequency while $I_{transmitter}$ is the current flowing on the transmitter coil. By using the value of mutual inductance from equation (1), the coupling coefficient, k can be calculated using equation (2) where L_1 and L_2 are inductance of primary and secondary coil respectively.

$$M = \frac{V_{induced}}{\omega I_{transmitter}} \quad (1)$$

$$k = \frac{M}{\sqrt{L_1 L_2}} \quad (2)$$

As there is an induced voltage introduced from the secondary coil to the primary coil, the total inductance of the WPT system would be changed as mutual inductance is involved. Based on Kirchoff Voltage Law for the aiding and opposing type of magnetic coupling, the sum of all voltages in this system can be calculated using equation (3).

$$V_L - L_{primary}\frac{di_{primary}}{dt} = \pm M \frac{di_{secondary}}{dt} \quad (3)$$

In the proposed study, the transmitter operates independently of receiver-side parameters. Therefore, reasonable assumptions are necessary to calculate the mutual inductance value:

a) The voltage change (loss or gain) across the primary coil is theoretically assumed to equal the mutually induced voltage in the secondary coil. Additionally, the mutual inductance is always treated as a positive value.

b) The mutual inductance is assumed to be slightly lower than its actual value, as the current in the primary circuit is typically less than that in the secondary circuit.

The transmitter cannot directly account for receiver-side parameters in real time. By assuming that the voltage change in the primary coil equals the mutually induced voltage in the secondary coil, the model avoids the need for additional complex measurements and ensures that the fundamental principle of electromagnetic induction is upheld. Furthermore, In practical wireless power transmission systems, the primary circuit's current is often lower than the secondary circuit's current due to efficiency factors and energy transfer characteristics. By assuming a lower mutual inductance value, the design remains conservative and accounts for possible losses, ensuring reliable operation under real-world conditions. Lastly, these assumptions reduce the complexity of analyzing mutual inductance in a system where only transmitter-side parameters are known. This is critical for designing and tuning the system without full knowledge of the receiver (or the load) as in the real-world scenario. Therefore, based on the two assumptions, a frequency range between 70kHz and 100kHz is used to perform frequency sweep analysis and obtain the voltage across the primary coil and current flow in the primary circuit. So, the value of mutual inductance can be calculated using equation (4).

$$M = \frac{\left|V_{transmitter} - L_{primary} I_{transmitter}\right|}{\omega I_{transmitter}} \quad (4)$$

Once the mutual inductance induced on the primary coil was found, this value would be used to estimate the frequency by using equation (5) where C is the capacitance.

$$f_{estimate} = \frac{1}{2\pi\sqrt{(L_{primary} + M)C}} \quad (5)$$

By including mutual inductance from the secondary coil into the system, it was more likely to see the system was operating at a resonance state. However, the frequency sweep analysis was conducted to investigate how a range of frequency approach to the new operating frequency where the mutual inductance was accounted for. Thus, the heatmap chart in the following section will be used to represent the frequency change for frequency sweep analysis while the mutual inductance changes with the current operating frequency also illustrated using a scatter graph. As one of the main objectives, the transmitted power was aimed to be further improved by accounting for mutual inductance from the secondary coil into the frequency estimation. After the frequency sweep analysis, the estimated frequency would be found when it has the least change from the current operating frequency. Then, this value will be used to compare with a resonant frequency that is calculated directly based on the specification of the inductor and capacitor using equation (6).

$$f_{resonant} = \frac{1}{2\pi\sqrt{L_{primary}C}} \tag{6}$$

Once the estimated frequency and resonant frequency were found, the measured voltage across the primary coil and measured current flow in the primary circuit would be used to calculate the transmitted power using equation (7).

$$P_{transmit} = V_{transmitter} * I_{transmitter} \tag{7}$$

To measure the improvement of the transmitted power, equation (8) is used to calculate how much percent changed or improved from the transmitted power when the resonant frequency was operated to the transmitted power when the estimated frequency was operated.

$$\text{Percentage change (\%)} = \frac{P_{estimated} - P_{resonant}}{P_{resonant}} * 100\% \tag{8}$$

4. RESULTS AND DISCUSSIONS

The frequency sweep analysis was done with an operating frequency in the range between 70kHz and 100kHz with different separation distances of coils (0cm, 2cm, 4cm and 6cm). The purpose of accounting mutual inductance into total inductance of the system was to estimate the operating frequency to make sure the transmitter always operated at a resonance state where the impedance of the series resonance is minimum as the reactance of the inductor has canceled the reactance of the capacitor. Based on Figure 5, it can be seen that the total inductance of the system would increase over the frequency for each separation of the coils. Except for the setup of 0cm separation distance where the total inductance of the system dropped after 89.0kHz. This is because losses from the skin effect and proximity effect affected the mutual inductance resulting in decrement in total inductance at higher operating frequency, especially when the coupling coefficient was high. However, these values of total inductance were then used to estimate the new frequency in frequency sweep analysis and displayed using heatmap charts as shown in Figure 6.

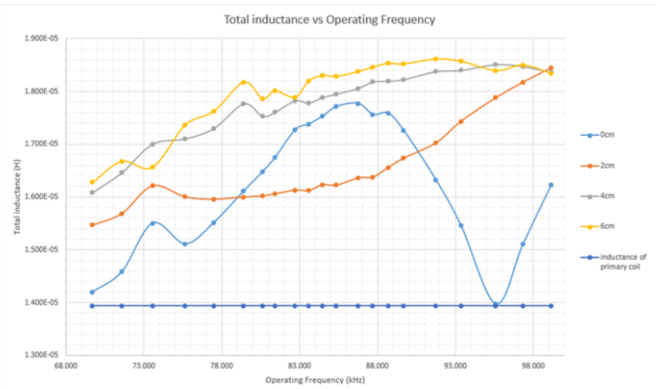

Figure 5: Total inductance changes

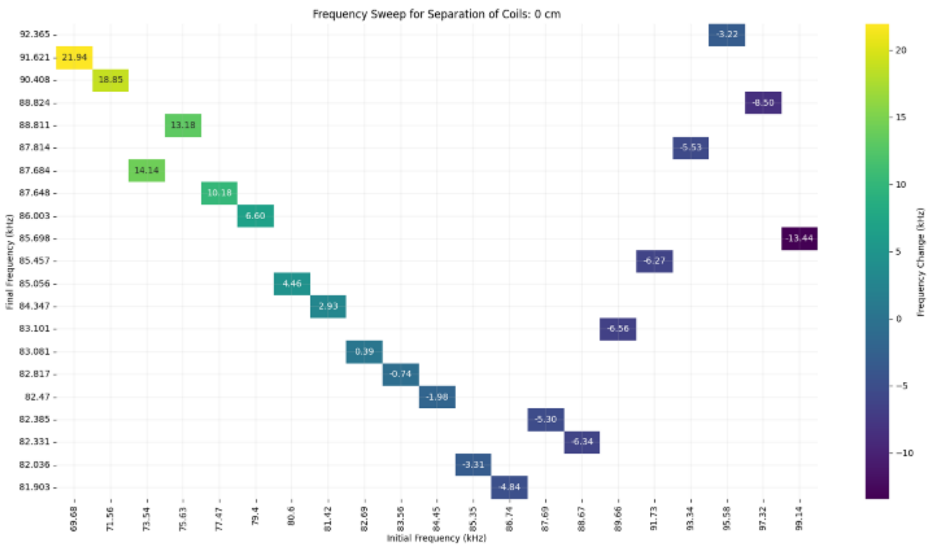
Frequency Sweep for Separation of Coils: 0 cm
Final Frequency (kHz)
Initial Frequency (kHz)
Frequency Change (kHz)
92.365
91.621
90.408
88.824
88.811
87.814
87.684
87.648
86.003
85.698
85.457
85.056
84.347
83.101
83.081
82.817
82.47
82.385
82.331
82.036
81.903
69.68
71.56
73.54
75.63
77.47
79.4
80.6
81.42
82.69
83.56
84.45
85.35
86.74
87.69
88.67
89.66
91.73
93.34
95.58
97.32
99.14
-3.22
21.94
18.85
-8.50
13.18
-5.53
14.14
10.18
6.60
-13.44
-6.27
4.46
2.93
-6.56
0.39
-0.74
-1.98
-5.30
-6.34
-3.31
-4.84
20
15
10
5
0
-5
-10

(a)

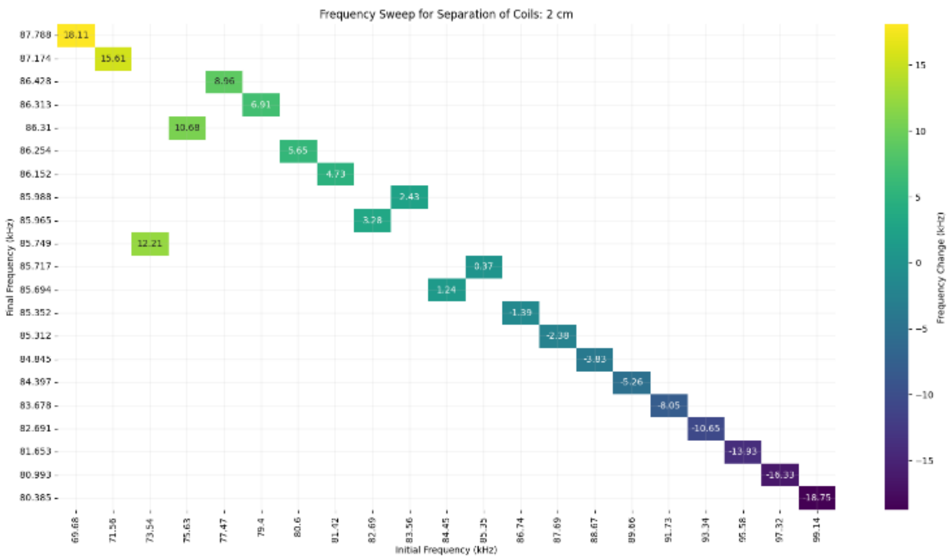
Frequency Sweep for Separation of Coils: 2 cm
Final Frequency (kHz)
Initial Frequency (kHz)
Frequency Change (kHz)
87.788
87.174
86.428
86.313
86.31
86.254
86.152
85.988
85.965
85.749
85.717
85.694
85.352
85.312
84.845
84.397
83.678
82.691
81.653
80.993
80.385
69.68
71.56
73.54
75.63
77.47
79.4
80.6
81.42
82.69
83.56
84.45
85.35
86.74
87.69
88.67
89.66
91.73
93.34
95.58
97.32
99.14
18.11
15.61
8.96
6.91
10.68
5.65
4.73
2.43
3.28
12.21
0.37
1.24
-1.39
-2.38
-3.83
-5.26
-8.05
-10.65
-13.93
-16.33
-18.75
15
10
5
0
-5
-10
-15

(b)

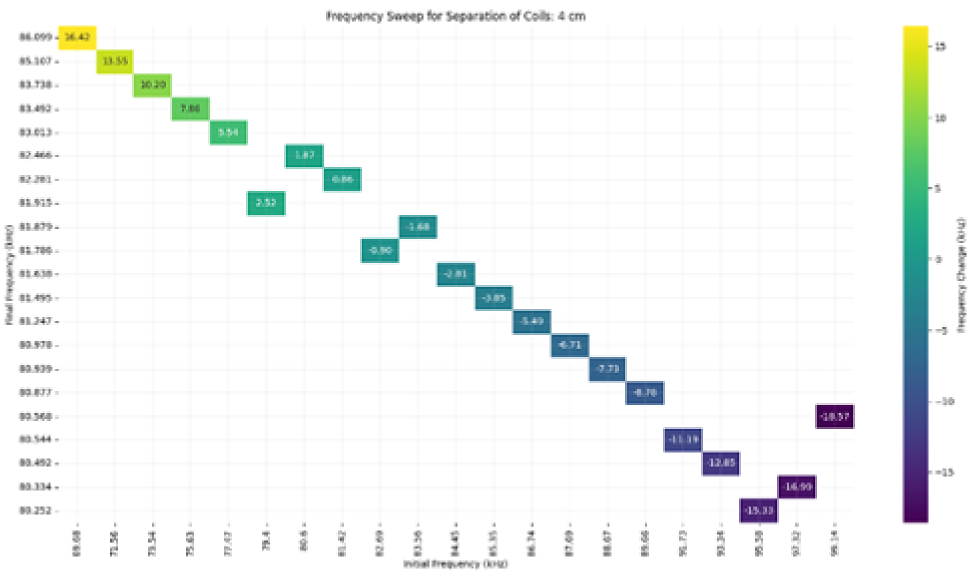
Frequency Sweep for Separation of Coils: 4 cm
Final Frequency (kHz)
Initial Frequency (kHz)
Frequency Change (kHz)
16.42
13.55
10.20
7.86
5.54
1.87
0.86
2.52
-1.68
-0.90
-2.81
-3.85
-5.49
-6.71
-7.73
-8.78
-18.57
-11.19
-12.85
-16.99
-15.33

(c)

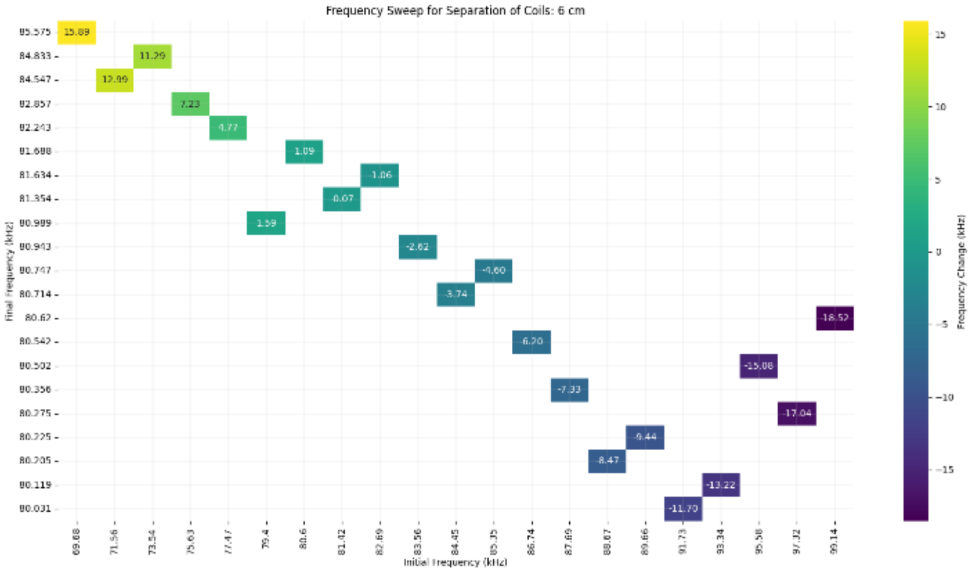

(d)

Figure 6: Frequency Sweep for separation distances of: (a) 0cm, (b) 2cm, (c) 4cm, (d) 6cm.

Based on Figures 6(a) to 6(d), the frequency estimation was done by picking the final frequency of that operating frequency with the lowest frequency change among the frequencies. Thus, Table 3 shows the estimated frequencies based on different separation distances between the coils.

Table 3: Estimated Frequencies

Setup / Distance between coils (cm)	Estimated frequency (kHz)
0	82.949
2	85.716
4	82.033
6	81.354

Following the frequency sweep analysis, the estimated operating frequency was determined by incorporating the mutual inductance of the hardware prototype. Concurrently, the resonant frequency calculated based on the circuit specifications was compared to the estimated frequency derived from the transmitted power measurements. The resonant frequency was identified as 92.463 kHz. Using these frequency values as references, the transmitted power was calculated, and the performance improvement was quantified as a percentage when the WPT prototype operated at the estimated frequency.

Table 4: Transmitted Power

Distance (cm)	Power (Watt)		Percentage change (%)
	Resonant Frequency	Estimated Frequency	
0	0.7749	1.3627	75.85
2	2.4925	3.0120	20.84
4	5.2216	5.7480	10.08
6	6.6454	6.7976	2.29

Based on Table 4, the theoretical calculation stated in Section II was capable of estimating a better operating frequency for better-transmitted power in a 4cm separation distance with at least 10% improvement. Not only that, the estimation was done with only parameter values from the transmitter side in contrast to prior studies that utilized static hardware configurations or complicated parameter adjustment methods. The frequency sweep analysis is essential for comprehending how various operating conditions—such as coil separation, mutual inductance, and the system's reactive characteristics—impact the overall transmission efficiency of the IWPT system. The study establishes a foundation for creating algorithms that may facilitate real-time adaptive tuning by gathering performance data across various operating frequencies.

5. CONCLUSION

Concluding the research, this paper proposed a theoretical calculation to estimate the optimal operating frequency that matches the resonant frequency for maximizing power transmission in IWPT systems. Both simulation software and a hardware prototype were deployed to test the proposed approach. The analysis conducted yielded significant findings where the estimated operating frequency improved power transmission by a minimum of 10% within a 4 cm distance, as outlined in Section 4. Having said that, the power transmission efficiency declined rapidly beyond this distance most likely due to the material of the copper wire used to construct the inductor which suffers from skin and proximity effects at higher frequencies. In conclusion, the study offers essential insights required for the implementation of self-adaptive tuning. It validates the correlation between mutual inductance and frequency optimization providing a definitive framework for a fully automated, efficient IWPT system in future advancements. The collected data is crucial for developing algorithms that enable the system to adapt in real-time, guaranteeing consistent performance in load variations.

ACKNOWLEDGMENT

The authors are extremely grateful to Universiti Teknikal Malaysia Melaka for their support, usage of the laboratory facilities and encouragement in completing this research

REFERENCES

[1] J. Van Mulders et al., Jul. 2022, “Wireless Power Transfer: systems, circuits, standards, and use cases,” Sensors, vol. 22, no. 15, p. 5573.

[2] J. Wang et al., Mar. 2024, “Design and analysis of an H-Type pickup for Multi-Segment wireless power transfer Systems,” Electronics, vol. 13.

[3] Y. Zhou, C. Liu, and Y. Huang, Jun. 2020, “Wireless Power Transfer for Implanted Medical Application: A review,” Energies, vol. 13, no. 11, p. 2837..

[4] L. Yang, X. Li, S. Liu, Z. Xu, and C. Cai, Feb. 2021, “Analysis and design of an LCCC/S-Compensated WPT system with constant output characteristics for battery charging applications,” IEEE Journal of Emerging and Selected Topics in Power Electronics, vol. 9, no. 1, pp. 1169–1180.

[5] N. Tesla, “Apparatus for Transmitting Electrical Energy,” US11119732, 1914..

[6] “Application of automatic resonant frequency tuning circuit to induction heating system,” IEEE Conference Publication | IEEE Xplore, Sep. 01, 2018.

[7] L. Shi, P. Alou, J. A. Oliver, J. C. Rodriguez, A. Delgado, and J. A. Cobos, “A Self-Adaptive wireless power transfer system to cancel the reactance,” IEEE Transactions on Industrial Electronics, vol. 68, no. 12, pp. 12141–12151, Dec. 2021, doi: 10.1109/tie.2020.3044817.

[8] A. Konishi, K. Fujiki, “Resonant Frequency Tuning System for Repeater Resonator,” IEEE Xplore, Sep. 2019.

[9] M. Ishihara, K. Fujiki, K. Umetani, and E. Hiraki, “Automatic Active Compensation Method of Cross-Coupling in Multiple-receiver Resonant Inductive Coupling Wireless Power Transfer Systems,” IEEE Xplore, Sep. 2019, doi: 10.1109/ecce.2019.8913279.

[10] M. Ishihara, K. Umetani, and E. Hiraki, “Automatic resonance frequency tuning method for repeater in resonant inductive coupling wireless power transfer systems,” 2018 International Power Electronics Conference (IPEC-Niigata 2018 -ECCE Asia), May 2018, doi: 10.23919/ipec.2018.8507768.

[11] R. Narayanamoorthi, “Modeling of capacitive resonant wireless power and data transfer to deep biomedical implants,” IEEE Transactions on Components, Packaging, and Manufacturing Technology, vol. 9, no. 7, pp. 1253–1263, Jul. 2019, doi: 10.1109/tcpmt.2019.2922046.
[12] J. M. Arteaga, S. Aldhaher, D. C. Yates, and P. D. Mitcheson, “A Multi-MHz Wireless Power Transfer System With Mains Power Factor Correction Circuitry on the Receiver,” IEEE Xplore, Mar. 2019, doi: 10.1109/apec.2019.8722038.
[13] G. Shi et al., “A sensorless Self-Tuning resonance system for piezoelectric broadband vibration energy harvesting,” IEEE Transactions on Industrial Electronics, vol. 68, no. 3, pp. 2225–2235, Mar. 2021, doi: 10.1109/tie.2020.2975457.
[14] K. Matsuura, D. Kobuchi, Y. Narusue, and H. Morikawa, “Communication-Less Receiver-Side Resonant Frequency Tuning Method for Magnetically Coupled Wireless Power Transfer Systems,” IEEE Xplore, Jan. 2021, doi: 10.1109/rws50353.2021.9360356.
[15] S. Mutlu, “Challenges in neural interface electronics: miniaturization and wireless operation,” in Elsevier eBooks, 2021, pp. 537–559.
[16] Cabrera, T.; Sánchez, J.A.A.; Longo, M.; Foiadelli, F. , November 2016, Sensitivity analysis of a bidirectional wireless charger for EV. In Proceedings of the 2016 IEEE International Conference on Renewable Energy Research and Applications (ICRERA), Birmingham; pp. 1113–1116.
[17] Sasatani, T.; Narusue, Y.; Kawahara, Y.; Asami, T, May 2017, DC-based impedance tuning method using magnetic saturation for wireless power transfer. In Proceedings of the IEEE Wireless Power Transfer Conference (WPTC), Taipei, Taiwan,; pp. 1–4.
[18] Saltanovs, R., May 2015, Multi-capacitor circuit application for the wireless energy transmission system coils resonant frequency adjustment. In Proceedings of the IEEE Wireless Power Transfer Conference (WPTC), Boulder, CO, USA.
[19] Xia, J.; Chen, D.; Wang, D.; Xu, D., December 2019, Analysis of Automatic Frequency Tuning for Wireless Power Transfer Systems. In Proceedings of the IEEE 4th Advanced Information Technology, Electronic and Automation Control Conference (IAEAC), Chengdu, China, 20–22.
[20] Sis, S.A.; Bicakci, S., October 2016, A resonance frequency tracker and source frequency tuner for inductively coupled wireless power transfer systems. In Proceedings of the 46th European Microwave Conference (EuMC), London; pp. 751–754.
[21] Kar, D.P.; Nayak, P.P.; Bhuyan, S.; Panda, S.K., 2014, Automatic frequency tuning wireless charging system for enhancement of efficiency. Electron. Lett., 50, 1868–1870.